

EVOLUTIONARY BIOLOGY

Cardiorespiratory interactions previously identified as mammalian are present in the primitive lungfish

Diana A. Monteiro,^{1,2*} Edwin W. Taylor,^{1,3*} Marina R. Sartori,⁴ André L. Cruz,^{2,5} Francisco T. Rantin,^{1,2} Cleo A. C. Leite^{1,2†}

The present study has revealed that the lungfish has both structural and functional features of its system for physiological control of heart rate, previously considered solely mammalian, that together generate variability (HRV). Ultrastructural and electrophysiological investigation revealed that the nerves connecting the brain to the heart are myelinated, conferring rapid conduction velocities, comparable to mammalian fibers that generate instantaneous changes in heart rate at the onset of each air breath. These respiration-related changes in beat-to-beat cardiac intervals were detected by complex analysis of HRV and shown to maximize oxygen uptake per breath, a causal relationship never conclusively demonstrated in mammals. Cardiac vagal preganglionic neurons, responsible for controlling heart rate via the parasympathetic vagus nerve, were shown to have multiple locations, chiefly within the dorsal vagal motor nucleus that may enable interactive control of the circulatory and respiratory systems, similar to that described for tetrapods. The present illustration of an apparently highly evolved control system for HRV in a fish with a proven ancient lineage, based on paleontological, morphological, and recent genetic evidence, questions much of the anthropocentric thinking implied by some mammalian physiologists and encouraged by many psychobiologists. It is possible that some characteristics of mammalian respiratory sinus arrhythmia, for which functional roles have been sought, are evolutionary relics that had their physiological role defined in ancient representatives of the vertebrates with undivided circulatory systems.

INTRODUCTION

In vertebrates, respiratory and cardiovascular systems are functionally linked and often exhibit tight interactions that optimize the delivery and removal of respiratory gases, producing coordinated responses to variations in metabolic demand or altered gas composition in the environment (1, 2). In mammals, one form of these cardiorespiratory interactions (CRIs) is respiratory sinus arrhythmia (RSA). This phenomenon is characterized by heart rate (f_H) increasing during inspiration and decreasing during expiration (3). Power spectral analysis (PSA) of f_H variability (HRV) reveals a peak at a relatively high frequency (HF), which is related to ventilation (4, 5). RSA is, in large part, mediated by fluctuations of the inhibitory input from the brain to the heart through the vagus nerve in response to both centrally generated (feed-forward) influences from respiratory neurons and afferent input from pulmonary stretch receptors (feedback) that gate baroreceptor inputs (6, 7). Beat-by-beat control is dependent on rapid conduction of bursts of efferent activity down the cardiac vagus, which contains myelinated “B-fibers” (7, 8). These CRIs are generated centrally by vagal preganglionic neurons (VPNs) and, in particular, cardiac VPNs (CVPNs), located primarily in the ventrolateral nucleus ambiguus (NA), where they interact with the ventral group of inspiratory neurons (1, 9–12). The existence of the NA and the central interactions generating RSA have been described from mammalian studies, and as a consequence, biomedical physiologists are apt to consider them uniquely mammalian, whereas a group of psychobiologists have erected a “polyvagal theory” that considers the mammals to have a “smart vagus,” denied

to other vertebrates, that provides a highly orchestrated set of physiological and behavioral functions (13). We have questioned the uniqueness of the structural and functional features of the mammalian cardiac vagus and its consequent role in the control of CRIs, as we consider these features to have evolved in the early phylogeny of the vertebrates.

This study set out to trace the evolutionary origins of mammalian RSA in the patterns of CRI typical of early air-breathing vertebrates by investigating its control in the South American lungfish (“piramboia”), *Lepidosiren paradoxa*. Lungfishes (Dipnoi) have previously been identified as a key group for the study of the evolution of the mechanisms that led to effective air breathing in vertebrates (11, 14). They are members of a group of lobe-finned fishes that constitute the Sarcopterygii, a group identified from a continuous fossil record originating in the Devonian period around 400 million years ago. The sarcopterygians split into two main lineages—the coelacanth that never left the oceans, presently represented by the “living fossil” *Latimeria*, and the rhipidistians that migrated into freshwater habitats. They, in turn, split into two major groups: the lungfishes and the tetrapodomorphs (15, 16). The lungfish evolved the first proto-lungs and proto-limbs, developing the ability to survive the temporary loss of their water environment, whereas the tetrapodomorphs migrated onto land to become committed air breathers, giving rise to present-day amphibians, reptiles, birds, and mammals. Thus, the lungfishes represent the earliest stages in the evolutionary record of air-breathing vertebrates. *L. paradoxa* has many plesiomorphic features characteristic of early tetrapods such as limb and jaw structure and an independent circulation for its primitive lung (16). *L. paradoxa* is the single representative of the Dipnoi in South America. It inhabits freshwater pools and slow-flowing rivers, which often contain very low levels of dissolved oxygen and are prone to dry out completely during dry seasons. The lungfish is an obligatory air breather, rising to the surface at regular intervals to ventilate its lung-like air-breathing organ (16), and can survive for long periods in burrows during drought. Thus, *Lepidosiren* depends almost exclusively on its lungs for O₂ uptake and shares a periodic breathing pattern with the tetrapod vertebrates.

¹Department of Physiological Sciences, Federal University of São Carlos (UFSCar), São Carlos, 13565-905 São Paulo, Brazil. ²National Institute of Science and Technology in Comparative Physiology (INCT FisComp), São Carlos, São Paulo, Brazil. ³School of Biosciences, University of Birmingham, Edgbaston, Birmingham B15 2TT, UK. ⁴Department of Zoology, São Paulo State University (UNESP), Rio Claro, São Paulo, Brazil. ⁵Institute of Biology, Federal University of Bahia (UFBA), Salvador, Bahia, Brazil.

*These authors contributed equally to this work.

†Corresponding author. Email: cleo.leite@ufscar.br

The aim of the present work was to study in detail the nature and control of the CRIs that occur during air breathing in *L. paradoxus*, to elucidate the role of the autonomic nervous system in generating these interactions, and to identify their functional characteristics. We hypothesized that furthering our understanding of these relationships in this primitive vertebrate may uncover their origins and present functional roles in mammals. The investigation encompassed physiological studies on unrestrained fish that used PSA of HRV plus ultrastructural and functional studies on the cardiac branches of the vagus nerve and neuroanatomical studies on the projections of the vagus nerve into the brainstem.

RESULTS

Recovery from surgery

After instrumentation, each animal was left in the respirometer to recover from the effects of anesthesia and surgery, as described in Materials and Methods. General recovery was attested as stabilization of cardiorespiratory and metabolic variables: mean heart rate (f_H), frequency of air breaths (f_R), O_2 uptake ($\dot{V}O_2$), and HRV (Figs. 1 and 2 and Table 1).

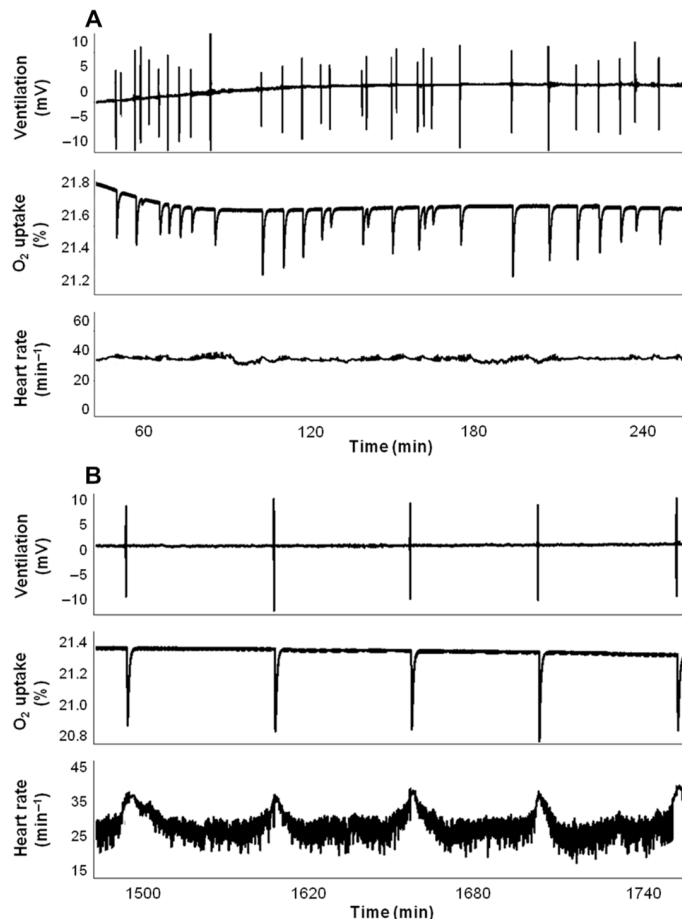


Fig. 1. Cardiorespiratory and metabolic recordings from a lungfish, *L. paradoxus*, at 25°C. Recordings of ventilation [recorded as surfacing events (mV)], oxygen uptake (measured as changes in % O_2), and heart rate (min^{-1}) during consecutive air-breathing cycles in a single lungfish (220 g). Recordings from 1 to 4 hours after surgery (A) and in the recovered, undisturbed animal 24 hours after instrumentation (B).

Cardiorespiratory parameters

When first inserted into the respirometer, the lungfish, *L. paradoxus*, showed elevated f_H (38 $beats\ min^{-1}$), with f_R both elevated (11 $respirations\ min^{-1}$; Table 1) and irregular (Fig. 1A shows these variables from 1 to 24 hours after instrumentation). When allowed to settle for over 24 hours, both f_H and f_R fell to lower stable levels (Table 1), with f_H showing regular, marked increases associated with each air breath (Fig. 1B). Undisturbed, recovered lungfish displayed a regular episodic breathing pattern (f_R , 1.7 $breaths\ hour^{-1}$). Mean tidal volume and duration of each exhalation and inhalation cycle (mean \pm SEM) were $25.3 \pm 5.1\ ml\ kg^{-1}$ and $10.7 \pm 1.2\ s$, respectively (Table 1). Mean f_H was stable, with a value of $29.7 \pm 1.0\ beats\ min^{-1}$, and O_2 uptake fell to a stabilized level (Fig. 2, A and B, and Table 1). O_2 uptake was restricted to the period of visits to the air-water interface, and heart rate increased markedly at each air breath (Fig. 1B). A tachogram of R-R intervals (RRi) revealed that they were relatively stable 6 hours after surgery but became variable and showed a marked reduction at each air breath after a recovery period of 24 hours (Fig. 2C). Recovery of HRV after 24 hours was accompanied by an increase in total power, as revealed by PSA to a stable high value (~ 575 to 975%) in comparison with immediately post-operative values (Fig. 2D and Table 1).

HRV and CRIs at rest in recovered fish

PSA of RRi in lungfish, following 24 hours of recovery, revealed pronounced RRi variation at each air breath identified as a large peak in the spectrum of PSA from each individual fish (Fig. 3, A and B, and fig. S1, A and B). These lungfish showed a clearly defined peak in the power spectrum at their individual breathing frequencies, demonstrating clearly defined CRIs. Because of the low respiratory rate of lungfish (in the range of 0.0003 to 0.0005 Hz, equivalent to 1.08 to 1.80 $breaths\ hour^{-1}$), the peaks are located at relatively “very low frequencies” (VLF), according to mammalian criteria (Task Force, 1996; see Materials and Methods). These respiration-related peaks likely incorporate other sources of variability, but the regular air breaths dominate the recordings.

Role of the autonomic nervous system in control of HRV

A tachogram of 8192 consecutive RRi from a single normal *L. paradoxus* (before drug injection; 48 hours after surgery) revealed a high level of HRV accompanied by a sharp reduction in cardiac interval at each air breath. Autonomic blockade reduced HRV and eliminated the changes associated with air breathing (Fig. 3, A and B). The effects of autonomic blockade on the mean of power spectra derived from eight lungfish are shown in Fig. 3B. Pharmacological blockade with atropine and propranolol reduced total PSD by about 2.5 times. There was no difference between atropine and double autonomic blockade.

The administration of atropine alone or when combined with propranolol significantly decreased HRV to levels similar to those measured in fish before their recovery from instrumentation. Consequently, the highest variance, SDNN, RMSSD, and total power were found in recovered fish 24 hours after instrumentation (Table 1).

The time course of changes in f_H at a series of air breaths was analyzed from recordings in eight lungfish following a 24-hour recovery. Instantaneous heart rate was recorded over 100 heartbeats around each air breath, and the beat-to-beat changes were related to the moment at which each fish exhaled before inspiring air. These data revealed a marked and rapid increase in mean f_H by 22%, from 29.5 ± 1.5 to 35.6 ± 1.8 at each air breath in normal, inactive fish (fig. S2, A and B). This increase seemed to be divided into two phases: an initial rapid increase in f_H at

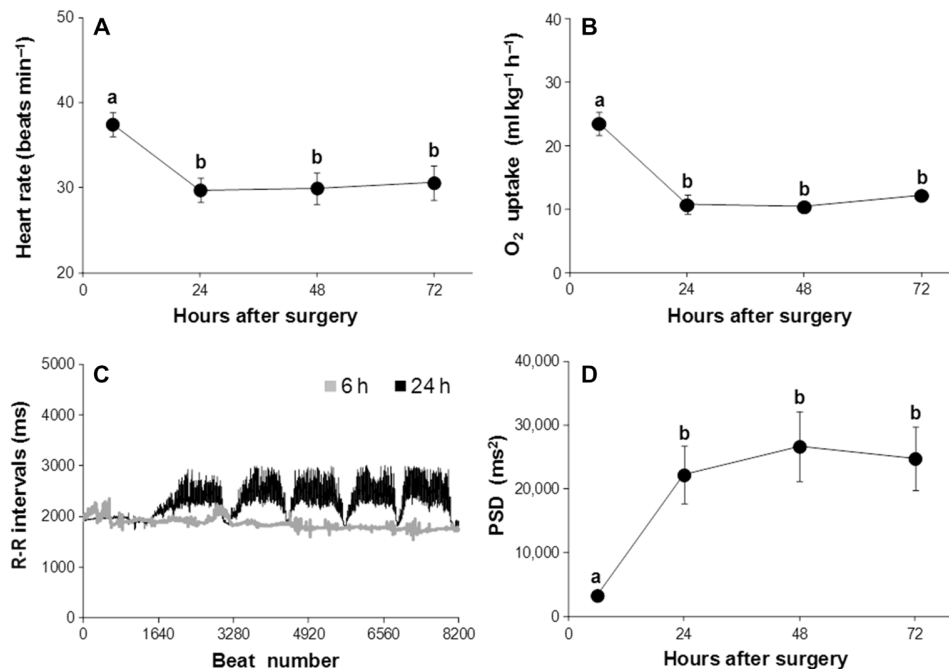


Fig. 2. Cardiac and metabolic indexes of recovery after instrumentation in lungfish, *L. paradoxus*, at 25°C. (A) Mean heart rate calculated from instantaneous electrocardiogram (ECG) recordings from eight lungfish 6 hours after implantation of electrodes and then every 24 hours for 72 hours. (B) Oxygen uptake from air for eight lungfish after 6, 24, 48, and 72 hours after surgical procedures. (C) A tachogram plot of 8192 consecutive RRi from a single *L. paradoxus* (196 g) 6 and 24 hours after surgery. (D) PSD derived from RRi collected from eight fish 6 hours after implantation of electrodes and then every 24 hours for 72 hours. Data in (A), (B), and (D) are plotted as means ± SEM. Different letters denote significant differences between mean values (ANOVA with Tukey's post hoc test, $P < 0.05$).

Table 1. Cardiorespiratory and HRV parameters in *L. paradoxus*. Experimental conditions: after instrumentation (Post-surgery; $n = 9$), recovered resting fish (Control; $n = 8$), with cholinergic receptor blockade (Atropine; $n = 6$), or total blockade of β -adrenergic and cholinergic receptors (Atropine + Propranolol; $n = 6$). Following instrumentation, lungfish was allowed to recover for at least 24 hours before measurements. Data are means ± SEM. Different superscript letters indicate significant differences [analysis of variance (ANOVA) with Tukey's post hoc test, $P < 0.05$]. SDNN, SD of all normal-to-normal intervals; RMSSD, square root of the mean squared differences between each successive RRi and the mean interval; PSD, power spectral density.

Parameters	Experimental groups			
	Post-surgery	Control	Atropine	Atropine + Propranolol
O ₂ uptake per breath (ml breath ⁻¹ kg ⁻¹)	0.11 ± 0.02 ^A	0.83 ± 0.07 ^B	0.29 ± 0.05 ^{A,C}	0.43 ± 0.08 ^C
$\dot{V}O_2$ (ml kg ⁻¹ hour ⁻¹)	23.6 ± 1.8 ^A	10.6 ± 0.8 ^B	24.2 ± 3.1 ^A	20.4 ± 2.5 ^A
f_R (breaths hour ⁻¹)	11.5 ± 1.7 ^A	1.7 ± 0.1 ^B	7.3 ± 1.5 ^C	5.9 ± 1.6 ^C
Tidal volume (ml kg ⁻¹)	27.9 ± 1.8 ^A	25.3 ± 1.6 ^A	26.7 ± 1.7 ^A	34.1 ± 1.9 ^B
Air-breathing cycle (s)	8.8 ± 0.4 ^A	9.5 ± 0.4 ^A	8.6 ± 0.3 ^A	9.7 ± 0.4 ^A
f_H (beats min ⁻¹)	38.8 ± 1.4 ^A	29.5 ± 1.5 ^B	39.2 ± 1.9 ^A	36.3 ± 2.2 ^A
RR mean (ms)	1547.4 ± 58.8 ^A	1,947.7 ± 74.7 ^B	1548.8 ± 69.8 ^A	1682.8 ± 90.4 ^A
RR variance (ms ²)	4953.2 ± 1187.8 ^A	28,244.1 ± 3,344.7 ^B	1834.9 ± 491.5 ^A	3690.9 ± 1311.4 ^A
SDNN (ms)	66.6 ± 8.1 ^A	192.4 ± 16.5 ^B	40.4 ± 6.3 ^A	54.9 ± 11.7 ^A
RMSSD (ms)	40.7 ± 4.2 ^A	102.8 ± 9.8 ^B	22.5 ± 5.5 ^A	19.9 ± 4.9 ^A
PSD (ms ²)	3664.0 ± 437.3 ^A	26,957.5 ± 2,791.1 ^B	998.9 ± 364.7 ^A	2903.7 ± 970.1 ^A

surfacing (within one heartbeat) and a further progressive increase in f_H during the breathing episode. Injection of the cholinergic receptor antagonist atropine into six lungfish eliminated beat-to-beat fluctuations and raised mean f_H to 39.2 ± 1.9. Total autonomic blockade, achieved by

injection of the β -adrenergic receptor antagonist propranolol, returned f_H to 36.3 ± 2.2 (fig. S2 and Table 1), the f_H value following an air breath before autonomic blockade (fig. S2), implying that a normal air breath is accompanied by suppression of autonomic tonic control.

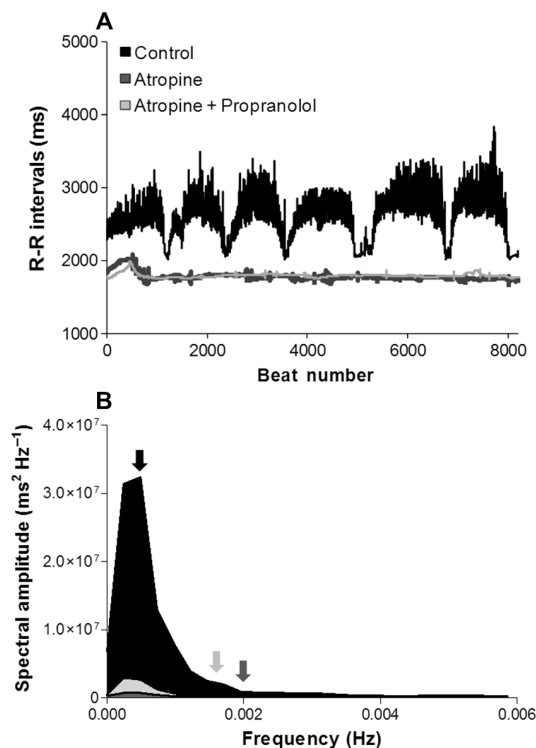


Fig. 3. Tachogram of RRi and power spectral density *L. paradoxus* at 25°C. (A) A tachogram plot of 8192 consecutive RRi from a single *L. paradoxus* (260 g) in untreated condition before drug injection (black trace) and following autonomic blockade with atropine (dark gray trace) and atropine + propranolol (gray trace). (B) Average spectral amplitude density from lungfish in an untreated condition (Control: before drug injection, 48 hours after surgery; $n = 8$, black area), after cholinergic receptor blockade (Atropine; $n = 6$, small dark gray area), and after total blockade of β -adrenergic and cholinergic receptors (Atropine + Propranolol; $n = 6$, small gray area). The mean breathing frequency (f_R) of the Control (f_R , ~ 1.7 breaths hour^{-1}), Atropine (f_R , ~ 7.3 breaths hour^{-1}), and Atropine + Propranolol (f_R , ~ 5.9 breaths hour^{-1}) groups are represented by black, dark gray, and gray arrows, respectively.

Resting and undisturbed lungfish exhibited a large cholinergic tonus of 32% and a relatively small adrenergic tonus of 7.5%, indicating that any increase in f_{HI} could be due to withdrawal of vagal tone. Hence, both the maintenance of mean f_{HI} and the modulation of RRi around each air breath show major dependence on vagal activity. This mechanism is evident in the effects of atropine injection on the elevation in heart rate and consequent abolition of the increase in RRi at each air breath in normal lungfish (Fig. 3 and fig. S2).

Following a 24-hour recovery from instrumentation, O_2 uptake per breath increased seven times compared to the value immediately after instrumentation. Autonomic modulation of RRi proved essential for normal levels of O_2 uptake, as injection of autonomic antagonists markedly decreased O_2 uptake per breath, by 65% after cholinergic receptor blockade and by 48% after total blockade (Table 1 and fig. S3).

Effects of changes in respiratory gas composition

The power spectrum representation of HRV and histogram of the breathing frequency of a *L. paradoxus*, following recovery from surgery, are presented in Fig. 4. The regularity of surfacing events for air breaths under normoxia resulted in clear coincident peaks in the histogram and power spectrum of HRV (Fig. 4, A and B). Following exposure to com-

bined hypoxia and hypercarbia, the frequency of air breaths markedly increased and became irregular (mean value, 11.2 ± 0.9 breaths hour^{-1} or ~ 0.0031 Hz; Fig. 4C). Also, mean tidal volume and duration of each exhalation and inhalation cycle were 80.1 ± 3.51 ml kg^{-1} and 19.8 ± 0.9 s, respectively, which represented significant increases by 3.3 and 2.1 times, respectively, when compared to the normoxic condition (recovery group, 24 hours after surgery; Table 1). So, exposure to a combination of hypoxia and hypercarbia caused an increase in respiratory drive and disruption of the regularity of air breathing. As a consequence, the characteristic respiration-related peak on the power spectrum for HRV disappeared. The spectrum presented a diffuse collection of peaks, scattered over the spectral bandwidth (Fig. 4D).

Conduction velocity and structure of the cardiac vagus

Peripheral electrical stimulation of the left cardiac branch of the vagus (at 24°C) evoked a compound action potential with a predominant fast component (9.0 to 10.5 m s^{-1}) plus discrete, considerably smaller and slower components (0.15 to 0.25 m s^{-1} ; Fig. 5A). These can be separated into “B-fiber” and “C-fiber” responses on the basis of mammalian criteria, with the slow components possibly recorded from the unmyelinated fibers identified in Fig. 5A that may be sensory fibers stimulated antidromically in this preparation.

Transmission electron microscopy (TEM) of serial transverse sections of the cardiac branch of the vagus nerve in *L. paradoxus* (Fig. 5, B and C) revealed the occurrence of large and small myelinated fibers, intermingled with bundles of unmyelinated ones. The mean values for the number and density of myelinated and unmyelinated fibers, their area and diameter, the percentage of occupancy of types, the mean myelin thickness, and the myelinated/unmyelinated fiber ratio are provided in table S1. There is a predominance of myelinated fibers in the cardiac vagus of *L. paradoxus*, as revealed by the ratio of myelinated/unmyelinated fibers. These fibers displayed relatively large diameters (up to 9.8 μm) and myelin thicknesses (up to 1.6 μm). Myelinated nerve fibers accounted for at least 55% of the tissue volume, and their distribution is not symmetric in a nerve section, constituting clusters of fast fibers. Myelinated fiber density and its percentage of occupancy in the nerve section were both significantly higher in the left cardiac branch, denoting a possible bilateral asymmetry of cardiac innervation. Unmyelinated fibers with fiber diameters ranging from 2.2 to 4.8 μm were equally distributed in the right and left cardiac vagus (table S1).

Neuroanatomy of VPN in the brain stem

Injection of the neural tracer fluorogold (FG) revealed VPN cell bodies distributed in four distinct locations in either side of the midline in the brainstem of lungfish (Fig. 6 and fig. S4A). Three of these locations were positioned close to the fourth ventricle, within the dorsal motor nucleus of the vagus (DVN): a large ventral group (DVNv), containing a total of 3000 labeled cells, extending from 12.4 mm caudal to 4.6 mm rostral to obex (Fig. 6, C and D, and fig. S4B). A smaller group of dorsal DVN (DVNd) formed by the separation of the large group of DVN midway through its rostrocaudal extent and found from 8 mm caudal to 4.8 mm rostral to obex, with a total of 300 cells (Fig. 6, B and D, and fig. S4C). Also, there is a separate, more rostral group characterized as the lateral DVN (DVNl) because of their location close to the much expanded fourth ventricle composed of 100 cells from 1.9 to 4.6 mm rostral to obex with a large number of cells in each section (4 to 20 cells; Fig. 6, A and D, and fig. S4D). The fourth location was composed of a group of smaller cells with a diffuse distribution ventrolaterally outside of the DVN, identified as scattered lateral vagal motoneurons (SLVNs)

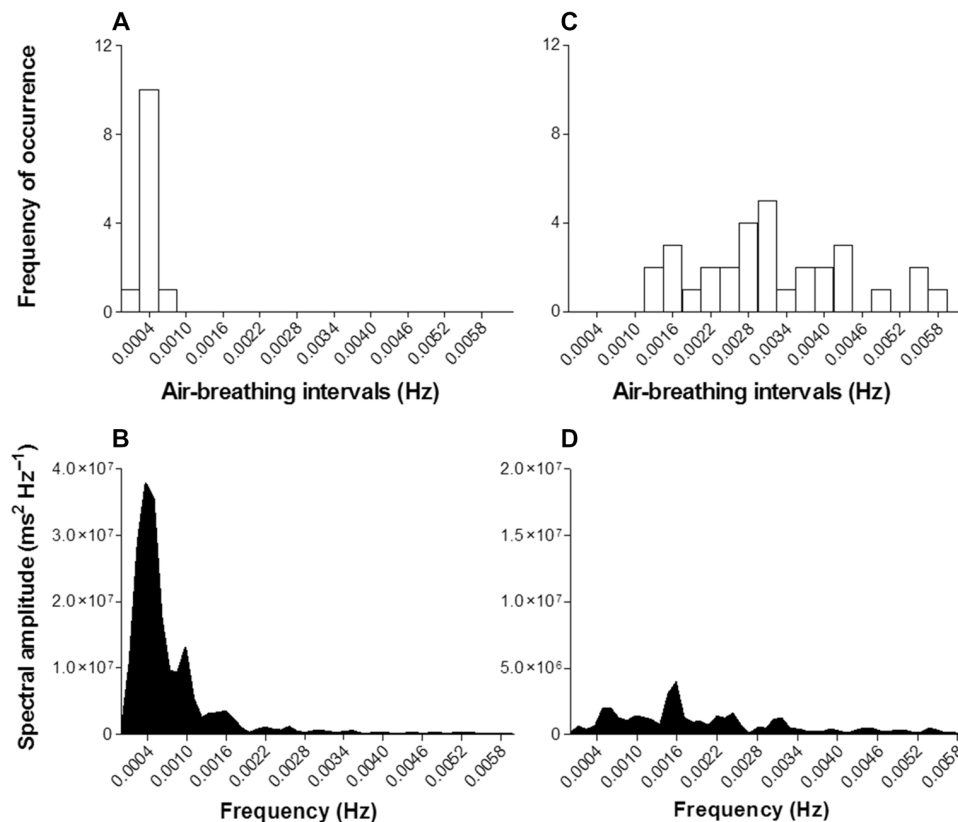


Fig. 4. Effects of hypoxia and hypercarbia on respiratory frequency and HRV in *L. paradoxus* at 25°C. Histograms of breathing frequency in 0.0006-Hz bins from a lungfish and HRV within 8192 consecutive heartbeat intervals under normoxia (263 g) (A and B) and hypoxia plus hypercarbia (gas mixture of 95% N₂, 5% CO₂, and 3% O₂) (318 g) (C and D). The spectra represent the relative distribution of frequency components within the HRV and breathing signals. The single, clear, respiration-related peak seen in the HRV signal from normoxic lungfish disappears from the lungfish under hypoxia plus hypercarbia due to the irregular nature of its air-breathing cycles. Spectral amplitude axes are up to 4×10^7 in (B) and 2×10^7 in (D).

and found from 4.9 to 6.0 mm rostral to obex, with a total of about 300 cell bodies (Fig. 6, B and D, and fig. S4E).

CVPN, labeled by DiI (1,1'-dioctadecyl-3,3,3',3'-tetramethylindocarbocyanine perchlorate) applied topically to the heart, constituted about 23% of the VPN-labeled cells (Fig. 6C). CVPNs were distributed from 3.4 mm caudal to 5.8 mm rostral to obex, partially overlapping the distribution of VPN (fig. S4, B to E). They were located within all cell groups described above, with CVPN constituting 20% of VPN in the DVNv, 67% in the DVNd, 6% in the DVNI, and 11% in the SLVN (fig. S4, B to E).

DISCUSSION

Morphological and paleontological evidence has long placed the lungfishes phylogenetically close to the origin of the lung-breathing tetrapod vertebrates. A recent study of limb regeneration has extended this evidence by revealing morphological steps similar to those seen in salamanders (17). These similarities are mirrored in the processes of differential gene expression that initiate and regulate limb regeneration in both groups. This recent evidence strongly supports the hypothesis that lungfish occupy the bona fide transition point from fish fin to tetrapod limb during the move onto land, and we have explored the complementary hypothesis that they have a primitive version of the control systems enabling effective air breathing that is conserved in tetrapod vertebrates, including mammals. Our investigation has revealed

that *L. paradoxus* has both structural and functional features controlling CRIs that have previously been considered solely mammalian.

Monitoring respiratory and cardiovascular variables over 72 hours revealed that recovery from the combined effects of anesthesia and instrumentation was complete after 24 hours. Recovery was assessed by stabilization of several factors: cardiorespiratory parameters (mean f_H and f_R), an index of metabolic rate ($\dot{V}O_2$), and HRV, which is an index of normal autonomic modulation of the heart. Analysis of HRV by PSA of RRi revealed that the highest variance, assessed as SDNN, RMSSD, or total power, was found in recovered fish 24 hours after surgery. A tachogram of RRi from a *L. paradoxus* 48 hours after surgery revealed a high level of HRV due largely to a sharp reduction in cardiac interval at each air breath. There was a clear peak in the spectrum for HRV at the air-breathing frequency for different fish. The marked rise in f_H at each air breath in settled, recovered *L. paradoxus* contrasts with measurements on other air-breathing fishes that typically show a sharp reduction in f_H at the moment of gulping air that precedes an equally sharp rise in f_H as they inflate the air-breathing organ (18). Our data reveal a two-stage increase in heart rate during an air breath that commenced at or immediately before surfacing. This implies that the initial increase is independent of inflation of the lung and is likely to be centrally generated.

Oxygen uptake per breath was low before recovery, whereas f_H , $\dot{V}O_2$, and air-breathing frequency were high. The high, unvarying f_H and increased f_R together constitute the immediate response of each

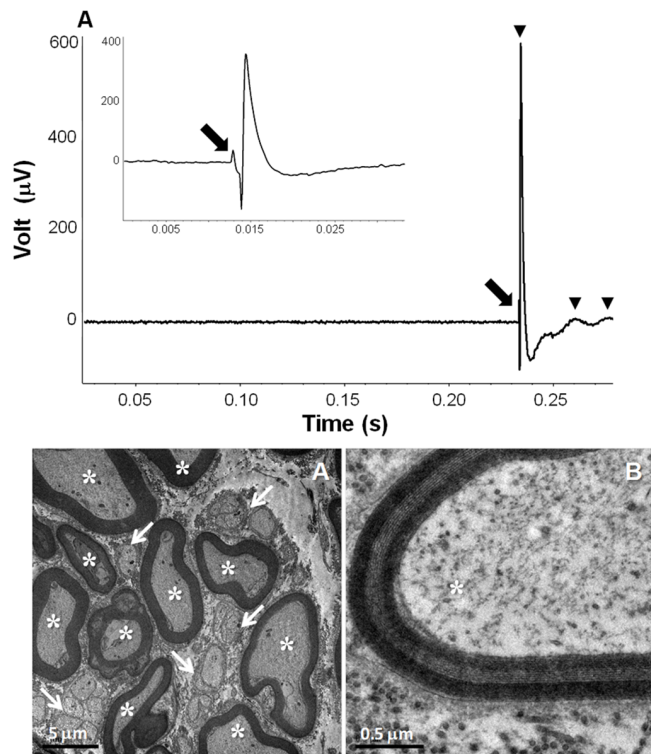


Fig. 5. Conduction velocity and transmission electron micrographs of cardiac vagus in *L. paradoxus* (505 g). (A) A typical example of a compound action potential recorded following electrical stimulation of the cardiac vagus nerve with a single pulse (0.5 ms, 70 V). Three components were identified (black arrowheads), with conduction velocities of 10.5, 0.23, and 0.16 m s⁻¹. Top left: Action potential recorded from an additional stimulation (0.5 ms, 50 V), recorded with a faster time base to identify the stimulus artifact (black arrow). (B) Photomicrographs obtained from the cross section of the cardiac vagus, which illustrates a representative range of fiber diameters. Arrows point to unmyelinated fibers, and asterisks indicate myelinated fibers. (C) The detail of the layering of the myelin sheath is readily observed.

fish to the stresses imposed by handling, anesthesia, and operative procedures. The increased $\dot{V}O_2$ may reflect a general increase in metabolic rate but, in part, will fuel the energy required for the frequent visits to the water surface. Following recovery, 24 hours after re-release into the holding tank, breathing frequency became slow and regular, and each breath was associated with a marked increase in both f_H and oxygen uptake per breath. Thus, the present study has provided evidence of a clear link between the marked acceleration in f_H at each air breath, identified in the analysis of HRV, and the consequent $\dot{V}O_2$ in unrestrained, settled lungfish. This increase in $\dot{V}O_2$ per breath in recovered lungfish represents an essential increase in efficiency (high rates of gas exchange in relation to work done) because the energy required to breathe is relatively high in air-breathing fishes that must gulp air from the water surface, using feeding muscles inserted on the pectoral girdle and innervated by the hypobranchial nerves (19, 20). Also, each visit requires energy for movement and orientation.

The infusion of atropine in *L. paradoxus* markedly elevated f_H to the rate achieved following an air breath, revealing a parasympathetic tonus of 32%, whereas the subsequent injection of propranolol revealed a sympathetic tonus of 8%. Virtually identical levels of cardiac autonomic tone were recorded from the African lungfish *Protopterus annectens* (21). Given the lack of adrenergic innervation of the lungfish heart (22, 23), the relatively low levels of adrenergic tone could be due to local

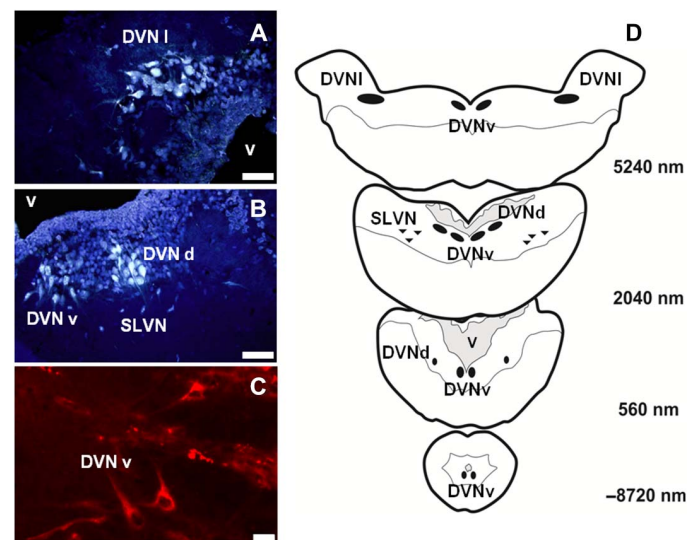


Fig. 6. Transverse sections and topographical illustration of the brainstem of the lungfish. (A to C) Micrographs of transverse 40- μ m sections of the brainstem rostral to obex, showing preganglionic motoneurons (VPN) labeled with the retrograde fluorescent tracer FG [(A and B) taken 4.9 and 2 mm caudal to 1 mm rostral to obex, respectively; scale bar, 50 μ m] and CVPN located by the retrograde transport of the fluorescent tracer Dil [(C) taken 2.1 mm rostral to obex; scale bar, 20 μ m]. There are three distinct cell groups (DVNv, DVNd, and DVNI) within the DVN and an SLVN. (D) Schematic diagram of VPN groups in the DVN in relation to the fourth ventricle (v). The cell bodies of VPN and CVPN were located in four groups. The main group comprised the ventrally located DVNv, which divided rostrally to form a separate dorsal subgroup (DVNd). This division merged again more rostrally. A third group of neuron cell bodies appeared at the rostral extent of the DVN (DVNI), and a scattered group of smaller cells was located ventrolaterally, outside DVN (SLVN). SLVN is homologous to the mammalian NA.

release of catecholamine from endogenous chromaffin cells, which line the atrial lumen (22, 23).

Autonomic blockade with atropine and propranolol elevated f_H and eliminated the changes associated with air breathing. The total power spectra were decreased by about 2.5 times, with HRV similar to that measured in fish before their recovery from surgery. So, the lack of HRV recorded 6 hours after surgery can be attributed to the loss of a predominant parasympathetic inhibitory tone, responsible for the loss of beat-to-beat control of f_H in the lungfish. The loss of autonomic control of the cardiovascular system commonly results from invasive instrumentation or anesthesia (24). In addition, exposure to experimentally induced hypoxia plus hypercarbia in *L. paradoxus* generated markedly irregular breathing cycles. The loss of the regular bouts of air breathing was accompanied by an increased f_H and by a decrease in the PSD of HRV from the levels characteristic of settled normoxic and normocapnic lungfish.

Our interpretation of the role of HRV in maximizing the oxygen uptake per breath must consider previous knowledge of the nature of peripheral control of perfusion of the dual respiratory gas exchangers in lungfish. Whereas heart rate increased during the intermittent ventilation of the lungs in both the South American and Australian lungfishes, *L. paradoxus* and *Neoceratodus forsteri*, in the African lungfish, *Protopterus* sp., there were very small changes in heart rate (25). However, in each of these species, pulmonary ventilation is associated with a marked rise in pulmonary blood flow, which is accomplished by vascular shunt control (25). Flow through the branchial

circulation is controlled by the ductus arteriosus, whereas perfusion of the lung is controlled by the pulmonary arterial vasomotor segment (PAVS), a muscular segment of the pulmonary artery with vasomotor activity (16, 23, 26, 27). Cholinergic stimulus dilates the ductus while constricting PAVS, indicating that both structures are controlled by cholinergic fibers, possibly of vagal origin (26, 28). During water breathing, cholinergic activation causes decreased pulmonary blood flow due to constriction of the pulmonary artery and dilation of both the ductus and brachial shunts, thus directing blood to the dorsal aorta and the branchial circulation (26, 29). During each air breath, a considerable portion of blood flow shifts from the systemic to the pulmonary circulation, with 20 to 70% of the total cardiac output directed to the lungs (30, 31).

Thus, CRI adjustments in f_H are an important part of a complex mechanism for the control of gas exchange that involves several cardiovascular adjustments, including venous return, myocardial contractility, net shunt control, and the control of perfusion in the respiratory tissue in the lungs. Notwithstanding the complex cardiovascular interactions underlying CRI, HRV is a fundamental part of it because it links directly with cardiac output. If the importance of the changes in f_H , expressed as peaks in the HRV spectrum at each air breath, is emphasized, then parallels between these change in CRI and similar respiration-related changes in CRI in other vertebrates can be compared. In water-breathing fish, perfusing a branchial circulation in series with the systemic circulation, several forms of CRI have been described, including cardiorespiratory synchrony, hypoxic bradycardia, or an increase in f_H during ram ventilation (1, 11, 32). In amphibians and reptiles, CRI is often associated with bouts of discontinuous ventilation, accompanied by cardiac shunt alterations (2, 33–35), whereas in mammals, CRI exists as RSA (1, 7, 11, 12, 20, 36).

Mammalian RSA shows an increase in f_H during inhalation and a reduction during expiration. It is more prevalent in healthy, fit individuals, arises close to term in fetal development, providing an indicator of normal development of the brainstem (11, 37), and is reduced in old age (5). All of these features imply a functional role in cardiorespiratory integration. Central control arises from changes in the activity of CVPN located outside of the DVN, in the ventrolateral NA (1, 7, 11, 12). In mammals, about 30% of VPNS, but up to 80% of CVPNs, are in the NA. Here, they are influenced by activity in the neighboring group of respiratory neurons that, in turn, are affected by afferent input from pulmonary stretch receptors that gate baroreceptor inputs (1). Activity in the respiratory neurons inhibits activity in CVPN, eliminating their tonic effect on the heart and causing the respiration-related changes f_H that constitute RSA (5, 7, 38). The beat-to-beat modulation of heart rate in mammals that constitutes RSA has been shown to be reliant on the rapid conduction velocity of efferent cardiac fibers arising from CVPN in the NA, conferred upon them by myelination (8). In mammals, myelinated/unmyelinated fiber ratios range from 1:3 to 1:7, and a larger diameter (up to 10 μm) is commonly reported for myelinated fibers (39, 40). The existence of dual locations for VPN outside of the DVN and, in particular, the location of CVPN in the ventrolateral NA, having myelinated efferent axons, have been considered uniquely mammalian, constituting their smart vagus and providing the physiological basis for the polyvagal theory recently reviewed by Porges (13).

However, these central interactions are not unique to mammals. In an elasmobranch fish, the dogfish, or catshark (*Scyliorhinus canicula*), CVPNs in the DVN show respiration-related activity that is driven rather than inhibited by activity in neighboring respiratory motoneurons (1, 11, 12, 19, 41, 42). The resultant respiration-related efferent activity

in the cardiac vagi is able to influence instantaneous f_H , generating cardiorespiratory synchrony. In *L. paradoxa*, each air breath is accompanied by an increase in heart rate, induced by a reduction in vagal tone, implying that activity in CVPN is inhibited during “inspiration,” as described in mammals. So, this primitive air-breathing fish has a control system generating CRI that is mammalian-like rather than piscine. The present study described VPN in four separate nuclei in the brainstem of *Lepidosiren*, all of them containing CVPN. All major groups were located in the DVN, but we describe a small group of VPN (identified as SVLN) in scattered locations ventrolateral to these groups that may constitute a primordial NA. Measurement of conduction velocities in the cardiac nerves revealed that a dominant component of the compound action potential had a high conduction velocity ($\sim 10 \text{ m s}^{-1}$), resembling the fast conducting B-fibers described from the mammalian vagus. Ultrastructural examination of transverse sections of these nerves revealed a large proportion of myelinated fibers. This representative of a primitive vertebrate group, with its origins located close to those of the tetrapods, has the structural and functional equipment that enables it to exert instantaneous, beat-to-beat control of the heart, which could be considered reasonably “smart.”

There is plenty of evidence for fine and rapidly exerted control of the heart in other nonmammalian vertebrates. Those with discontinuous breathing patterns, such as air-breathing fish or diving tetrapods, typically display bradycardia during apnea and a pronounced cardiac acceleration immediately upon the first air breath, implying overriding central nervous integration of their cardiorespiratory systems (10, 11). The increased heart rate immediately at the onset of periodic air breathing results mainly from withdrawal of vagal activity to the heart due to central interactions between motor neurons driving both systems (1, 11). The rapid response with a marked tachycardia often developing between two heartbeats implies a B-fiber response dependent on myelinated efferent fibers. Data from *S. canicula* (41, 42) showed that the cardiac vagus exhibited conduction velocities between 4.75 and 16.3 m s^{-1} similar to those described as B-fibers in mammals (10, 32). Myelination of the vagal branches has been described in fish, mammals, and birds (5, 40–43). Two locations for CVPN were described for *S. canicula*, with those in DVN showing respiration-related activity that could recruit the heart into cardiorespiratory synchrony, whereas a scattered ventrolateral group showed sporadic activity linked to hypoxic bradycardia (32, 42). The proportion of VPN located outside of the DVN varies markedly between groups of nonmammalian vertebrates, from 30 to 40% in some amphibians and reptiles, whereas in fish, other reptiles, and birds, it can be as low as 2 to 5% (11, 20). This may reflect the relative importance of central, feed-forward versus reflex, feedback control exerted on the heart via the vagus nerve (11, 12).

Porges (44) has promoted the polyvagal theory, ascribing to it many behavioral and even social functions in humans such as “love.” We do not wish to intervene in the debate around these extensions of the polyvagal theory; however, we do contest its physiological basis and evolutionary assumptions. According to Porges (13), CVPN originating in the NA and supplying the heart with myelinated efferent axons, having high conduction velocities, constitutes the smart vagus restricted to mammals, whereas the “lower” vertebrates retain the ancient vagus, restricted to the DVN and supplying unmyelinated, slow fibers that generate slowly developing, defensive changes in heart rate. He identifies a phylogenetic progression from the regulation of the heart by endocrine communication, to unmyelinated nerves, and finally to myelinated nerves found exclusively in mammals (13) and persists in stating that “only mammals have a myelinated vagus,” linking this to

the evolution of the NA (13). The present study reveals that the mechanisms he identifies as solely mammalian are undeniably present in the lungfish that sits at the evolutionary base of the air-breathing vertebrates. These include (i) a predominant role for vagal control of heart rate, as described for many other vertebrates, including mammals; (ii) close coupling between respiration and heart rate recorded as instantaneous changes in heart rate due to changes in vagal control at the onset of each air breath, detected by using PSA to characterize HRV; (iii) efferent vagal fibers with fast conduction rates (similar to mammalian B-fibers) conferred upon them by myelination; and (iv) CVPN, responsible for controlling heart rate via the parasympathetic vagus nerve having multiple locations within the dorsal vagal motor nucleus, plus scattered cells in a more ventrolateral location that could conceivably be a primordial NA. Together, these enable interactive control of the circulatory and respiratory systems, similar to that described for tetrapods, including mammals. A closer examination of the available literature reveals that other groups of vertebrates also presage the mechanisms required for fine control of heart rate (1, 11). Several authors have shown that HRV related to respiration is present in species of amphibians (2), reptiles [for example, rattlesnakes (45)], and birds [ducks (10, 11) and shearwaters (43)]. Thus, the repeated contention, central to the polyvagal theory, that the structural and functional bases of RSA are solely mammalian is clearly fallacious.

It has been suggested that RSA or HRV in synchrony with respiration may increase the effectiveness of pulmonary gas exchange in mammals by matching perfusion to ventilation within each respiratory cycle (5, 46). Although there is robust evidence that the incidence of a clear RSA is correlated with health, age, and several particular cardiovascular problems in human subjects (47–49), we have lacked direct experimental evidence of its physiological role. Hayano *et al.* (50) developed a model of RSA in anesthetized dogs to examine the hypothesis that RSA improves the effectiveness of pulmonary gas exchange. The authors demonstrated that artificial RSA could decrease the ratio of physiological dead space to tidal volume and the fraction of intrapulmonary shunt by 10 and 51%, respectively, and increase O₂ consumption by 4% compared with control. This small improvement obtained from such an extreme preparation does not support a clear physiological role for RSA in the normally functioning mammal. By contrast, the present data from lungfish show that HRV maximizes oxygen uptake per breath in settled, normal animals, indicating a positive influence on gas exchange at the level of the lung via effective ventilation/perfusion matching.

It is possible that investigation of a clear functional role for RSA in mammals failed to experimentally record an important quantitative improvement in gas exchange because of the completely divided circulation, characteristic of the group. This possibility invites a provocative evolutionary hypothesis: that RSA in mammals is a primitive character with a minimal quantitative role in respiratory gas exchange because their completely divided circulation obviates a cardiac or circulatory shunt between systemic and pulmonary circulations. In air-breathing vertebrates having undivided circulations, the elevated heart rate during inspiration is accompanied by a reduction in the peripheral resistance of the lung circuit (both under vagal control), causing increased perfusion and exchange of respiratory gases over the lung. This does not refute the alternative hypothesis that RSA in mammals can save cardiac work. While disputing the evidence for RSA improving respiratory gas transport, Ben-Tal *et al.* (51), using complex modeling procedures, raised the idea that RSA could minimize cardiac work while maintaining physiological levels of the partial pressure of CO₂. Thus, it is possible

to propose that the changes in heart rate observed during inspiration and characterized as RSA can only play a substantial role in improving the effectiveness of respiratory gas exchange over the lung in non-mammalian, non-avian species, having an undivided circulation with a functional cardiac or circulatory shunt. Hence, until further experimental validation, we cannot refute the hypothesis that RSA may be a relic character in mammals that has been retained over evolutionary time, having a rather limited role in improving respiratory gas exchange in fit, young individuals while providing some degree of protection by reducing cardiac work. Thus, the present study has illustrated that, apparently, highly evolved control systems can have primitive roots. This finding should give pause for thought to many biomedical physiologists and, in particular, to a faction within psychobiology (13), questioning their often anthropocentric assumptions.

MATERIALS AND METHODS

Animals

Specimens of piramboia, the South American lungfish, *L. paradoxus*, of either sex and a mean body mass of 0.26 ± 0.2 kg (mean \pm SD) were obtained from commercial suppliers in Mato Grosso do Sul, Brazil. The fish were transported to a holding facility in the Department of Physiological Sciences, Federal University of São Carlos (UFSCar), São Carlos, São Paulo state, Brazil, where they were maintained indoors, in 500-liter holding tanks, supplied with a flow of well water at $24 \pm 2^\circ\text{C}$, under controlled photoperiod (12 hours:12 hours). The fish were fed to saturation every 2 days with fish pellets (40% of protein) but were fasted for 48 hours before use in experiments. This study was performed with the approval of the Committee of Ethics in Animal Experimentation (CEUA; approval no. 2032180216) of UFSCar and in accordance with national guidelines for the care and use of laboratory animals.

Physiological experimentation: Surgery, recovery, and recording conditions

The fish used for cardiorespiratory recording were anesthetized by immersion in a solution of benzocaine (0.5 g liter⁻¹) and then placed on a surgical tray with access to air for breathing with the gills irrigated by a flow of water containing the anesthetic (0.25 g liter⁻¹). Using sterile techniques, two ECG electrodes were inserted under the skin in the ventral midline: one just anterior to the heart and the second electrode approximately 2 to 3 cm caudal to that position and posterior to the heart. Electrodes and wires were secured on the skin by cotton sutures. Lidocaine (2%) was injected at the site of electrode insertion. The procedure took about 5 min. Recovery from anesthesia was achieved by gill/skin irrigation with anesthetic-free water. After recovery of righting reflexes and normal movement, each fish was released into anesthetic-free water with access to air to complete recovery (20 to 30 min). Each fish was then placed in a purpose-built respirometer with both aquatic and aerial phases. The chamber contained 7 liters of continuous flow normoxic water (140 mmHg) maintained at 25°C . The fish had open access from the water surface to an air space (200 ml) composed of a translucent plastic funnel attached to the top of the respirometer. Recordings started 1 hour after each fish was placed into the respirometer.

The experiments were conducted with the aim of monitoring settled fish, showing routine levels of activity. Mean heart rate (f_H), oxygen uptake ($\dot{V}O_2$), and HRV were recorded continuously for 8 to 10 hours each day for up to 3 days to follow and evaluate the time course of recovery from instrumentation. The experimental protocol was followed

on fish reckoned as fully recovered from anesthesia and the operative procedures, based on the overall metabolic and autonomic indices, reflected by $\dot{V}O_2$ and HRV.

Recordings of cardiorespiratory parameters

The ECG was recorded at 1 kHz, amplified and filtered using a bioamplifier and data acquisition unit (PowerLab system, ADInstruments), and used as a measure of mean f_H . Instantaneous f_H was calculated from RRi on the ECG waveform and used to obtain the sequence of intervals required for derivation of HRV, as described in the following sections.

To record the incidence and volume of air breaths, a Fleisch tube (pneumotachograph) connected to a differential pressure transducer [adapted from Glass *et al.* (52)] was connected to the open end of the funnel. The air chamber was continuously flushed at 400 ml min⁻¹ via a mass flow controller (Sable Systems International). The excurrent air passed through columns of Drierite (Sigma-Aldrich) and an O₂ analyzer (FC-10A; Sable Systems International). All signals were recorded continuously by a data acquisition system (ADInstruments) and used to calculate the frequency of air breaths (f_R) and O₂ uptake per breath.

Heart rate variability

To characterize HRV using PSA, the raw ECG signal was converted into a tachogram of RRi from a continuous trace consisting of 8192 consecutive heartbeats, containing no artifacts. This long time series was necessary to assemble proper recordings of variations in RRi through 6 to 10 consecutive ventilatory cycles ($f_R = 1$ to 2 respirations hour⁻¹, 0.0003 to 0.0005 Hz, in resting normoxic lungfish at 25°C). The sequence of RRi was analyzed using purpose-built software (CardioSeries v.2.6.2, www.danielpentead.com) designed to perform time-frequency analysis of cardiovascular variability, allowing precise adjustment of parameters related to frequency domain analysis (for example, interpolation rate, segment length, and boundaries of frequency bands), using a Hanning window to minimize spectral leakage and interpolated at 2 Hz. The spectrum of variability was calculated for segments of data using a direct fast Fourier transform algorithm for discrete time series. HRV was represented on both time and frequency domains, and variability was quantified by the average SDNN and RMSSD. The spectra were also integrated for total PSD. Nonstationary data were not taken into consideration for PSD calculation. Spectral integration for the separation of LF and HF bands has no relation to the three main spectral components distinguished in the PSA spectrum from resting humans, which are HF (0.15 to 0.4 Hz), LF (0.04 to 0.15 Hz), and VLF (0.003 to 0.04 Hz) (37). So, band separation was not considered. The resultant output is plotted graphically, where cyclic oscillations in f_H appear as peaks at their relative oscillatory frequencies in the power spectrum.

CRIs in recovered fish

After recovery from instrumentation, mean routine levels of cardiorespiratory variables were recorded from a continuous trace of 10 to 12 hours. Fish were then subjected to pharmacological blockade of sympathetic and parasympathetic influences on f_H . On the fourth day of recording, atropine sulfate (1.2 mg kg⁻¹) (Sigma-Aldrich) was injected into the peritoneal cavity to block muscarinic receptors (21). Subsequently, on the fifth day of recording, atropine plus propranolol (2.7 mg kg⁻¹) (Sigma-Aldrich) was injected to block cholinergic and β -adrenergic receptors (21). The drugs were dissolved in 0.9% sterile saline. The maximum bolus injection volume was 1 ml kg⁻¹. The cholinergic and adrenergic tones on the heart were calculated from combined mean RRi for individual fish (45).

CRIs on exposure to hypoxia and hypercarbia

To further explore the cardiac responses to air breathing observed by PSA of RRi, we generated alterations in ventilation by chemoreceptor stimulation. Following recovery in HRV under normoxic conditions, the air space in the experimental chamber was gassed with a preformulated mixture of 3% O₂, 2% CO₂, and 95% N₂ (São Carlos Gases) delivered through a gas flow meter at 400 liters min⁻¹. The alterations in f_H were plotted as interval histograms. Although air-breathing vertebrates are seldom exposed to aerial hypoxia and hypercarbia, experimental exposure to varying gas mixtures is a common method used to induce changes in f_H (53, 54). The procedure aimed to evoke changes in ventilation, making it possible to validate that the LF peak revealed by PSA on normoxic lungfish was a result of CRIs.

Measurement of conduction velocity

Reflex control of heart rate requires close coordination between afferent and efferent arms of reflex arcs and its connections in the central nervous system. Hence, of greatest importance in the beat-to-beat control of the heart is rapid conduction of activity in the efferent (motor) arm of the reflex. The conduction velocities of the efferent axons in the cardiac nerves of the lungfish were measured in vivo in decerebrated lungfish. The cardiac vagus was exposed close to the pericardium by a lateral incision, dissected free of connective tissue, and mounted on bipolar silver electrodes for recording. The electrodes were connected via a headstage to a biological amplifier (Neuro Amp EX, PowerLab, ADInstruments). The vagus nerve was then sectioned cranially, close to the brainstem, and raised onto a pair of platinum hook electrodes connected to a physiological stimulator (Grass S48, Grass Medical Instruments). Diverse bursts of pulses of electrical stimulation (duration, 0.2 to 1.5 ms; 5 to 70 V) were delivered downstream at 20-s intervals. The velocity of the compound potentials generated in the nerve was calculated based on the time lapse between the artifact caused by stimulation and the nerve's response, with reference to the length of the nerve between the points of stimulation and recording (63 mm). These electrical recordings were performed inside a screened metal "Faraday" cage to reduce electrical interference with the recorded signals. Recording sample rate was set at 40 kHz.

Transmission electron microscopy

Conduction velocities in nerve fibers relate to their diameter and, for rapid conduction, to the presence of myelination (55). To count the numbers of vagal fibers and to record the incidence of myelinated fibers in the cardiac vagus, the right and left branches were dissected out of a fish under terminal anesthesia and fixed in Karnovsky's solution [2.5% glutaraldehyde and 2% paraformaldehyde in 0.1 M cacodylate buffer (pH 7.4)] and postfixed in 1% osmium tetroxide, 0.8% potassium ferrocyanide, and 5 mM calcium chloride in 0.1 M sodium cacodylate buffer (pH 7.4) for 1 hour. Portions of the fixed nerves were washed three times for 10 min each in the same buffer and dehydrated in a graded series of acetone, followed by three successive baths of 100% acetone and subsequent replacement of the acetone with Polybed resin (1:1) for 6 hours. Ultrafine sections of around 80 nm were obtained using an automatic ultramicrotome (Leica EM UC7) and collected with 200-mesh copper grids. The sections were then treated with uranyl acetate and lead citrate to increase contrast (56). Photomicrographs were obtained using a transmission electron microscope (JEOL 1230 TEM). These images were analyzed by dedicated software (ImageJ) to measure the area, major fiber diameter, myelin thickness, and number of myelinated and nonmyelinated fibers. The density of the unmyelinated or

myelinated fibers and the ratio of myelinated/unmyelinated fibers were calculated, including the percentage of the nerve area occupied (percentage of occupancy) by the unmyelinated and myelinated fibers.

Neuroanatomy

Having shown that central control of variations in heart rate is exercised predominantly by the parasympathetic arm of the autonomic nervous system, with efferent supply provided by the Xth cranial nerve, the vagus, we traced its projections into the brainstem. Fluorescent tracers were used to map the distribution of VPN in the brainstem. For retrograde labeling of VPN, FG (hydroxystilbamidine bis-methanesulfonate; Sigma-Aldrich) was dissolved in sterile saline at 3 mg ml⁻¹ (57), and a volume of 5 µl g⁻¹ of the solution was injected intraperitoneally. The animals were then kept in holding tanks under routine conditions (see above) for 70 days at 24°C to enable transport of the tracer along the axons and its accumulation in the vagal neuron cell bodies.

To locate the areas in the brainstem containing CVPN, DiI (Sigma-Aldrich) was topically applied to the heart, as described by Corbett *et al.* (58). Following anesthesia, as described above, the pericardial sac was exposed, and a 3- to 4-mm piece of sterile hemostatic sponge impregnated with DiI crystals (0.5 mg) was placed on the heart, close to the sinoatrial node region, and secured in place by suturing the pericardium. Each animal was then recovered from anesthesia and returned to a holding tank for a period of 40 days, during which the tracer was transported to cell bodies of CVPN in the brainstem. Lungfish brains were fixed, as described below.

Fish from either protocol were then anesthetized with benzocaine and perfused transcardially, first with heparinized saline solution and then with 4% paraformaldehyde in 0.1 M sodium phosphate buffer at pH 7.4. The brain and the initial portion of the spinal cord were carefully dissected out and stored in the fixative solution for up to 8 hours at 4°C. The sample was then washed with buffered saline and placed overnight in 20% sucrose phosphate-buffered solution as a cryoprotectant at 4°C. Each brain was then frozen and sectioned (transverse sections of 40 µm) on a cryostat (Microm HM 505 E), and serial sections were mounted on gelatin-coated slides, coverslipped over glycerine. Sections were examined under a photomicroscope (Olympus BX50 illuminator UV U-ULH) with a video camera attached to an image analysis system (Image-Pro Plus), enabling the images of fluorescing neuron cell bodies to be captured. Cell bodies of labeled neurons were counted and mapped according to their proximity to the fourth ventricle and their rostrocaudal distance from obex, the point on the brainstem from which the rostral extent of the fourth ventricle is covered dorsally by the choroid plexus that contains no nervous tissue. We report the results of the distribution of VPN and CVPN neurons from specimens, providing the highest cell counts following application of FG or DiI.

Analysis of data

Cardiorespiratory and HRV parameters are presented as means ± SEM. One-way ANOVA complemented by Tukey's multiple comparison test (GraphPad Instat version 3.00, GraphPad Software) was performed to check the possible existence of significant variations between the values obtained at different times in recovery protocol or to verify the occurrence of possible differences among experimental groups (Control, Atropine, and Atropine + Propranolol groups). Morphometric data from the vagus nerve were tested using the unpaired Student's *t* test, with the variables being between the right and left side. All assumptions to perform the statistical analysis were taken into account

(that is, independence, normality, and homoscedasticity). All differences between means at a 5% ($P < 0.05$) level were considered significant. For clarity, the number of animals used in each procedure is indicated in the relevant figures and tables.

SUPPLEMENTARY MATERIALS

Supplementary material for this article is available at <http://advances.sciencemag.org/cgi/content/full/4/2/eaag0800/DC1>

fig. S1. Spectral amplitude density from two lungfish (*L. paradoxus*) with different breathing frequencies.

fig. S2. Changes in the heart rate in *L. paradoxus* during an air-breathing event at 25°C.

fig. S3. The effect of autonomic modulation of HRV on mean oxygen uptake per breath in *L. paradoxus* at 25°C.

fig. S4. The rostrocaudal distribution of cell bodies of VPN in the brainstem of *L. paradoxus*.

table S1. Morphometric variables in the ultrastructure of transverse sections of the cardiac branches of the vagus nerve in *L. paradoxus*.

REFERENCES AND NOTES

1. E. W. Taylor, D. Jordan, J. H. Coote, Central control of the cardiovascular and respiratory systems and their interactions in vertebrates. *Physiol. Rev.* **79**, 855–916 (1999).
2. T. Wang, M. S. Hedrick, Y. M. Ihmied, E. W. Taylor, Control and interaction of the cardiovascular and respiratory systems in anuran amphibians. *Comp. Biochem. Physiol. A Mol. Integr. Physiol.* **124**, 393–406 (1999).
3. A. J. Garcia, J. E. Koschnitzky, T. Dashevskiy, J. M. Ramirez, Cardiorespiratory coupling in health and disease. *Auton. Neurosci.* **175**, 26–37 (2013).
4. J. A. Hirsch, B. Bishop, Respiratory sinus arrhythmia in humans: How breathing pattern modulates heart rate. *Am. J. Physiol.* **241**, H620–H629 (1981).
5. P. Grossman, E. W. Taylor, Toward understanding respiratory sinus arrhythmia: Relations to cardiac vagal tone, evolution and biobehavioral functions. *Biol. Psychol.* **74**, 263–285 (2007).
6. D. L. Eckberg, Human sinus arrhythmia as an index of vagal cardiac outflow. *J. Appl. Physiol.* **54**, 961–966 (1983).
7. D. Jordan, K. M. Spyer, Central neural mechanism mediating respiratory-cardiovascular interactions, in *Neurobiology of the Cardiorespiratory System*, E.W. Taylor, Ed. (Manchester Univ. Press, 1987), pp. 322–341.
8. J. F. X. Jones, Y. Wang, D. Jordan, Heart rate responses to selective stimulation of cardiac vagal C fibres in anaesthetized cats, rats and rabbits. *J. Physiol.* **489**, 203–214 (1995).
9. D. Jordan, M. E. M. Khalid, N. Schneiderman, K. M. Spyer, The location and properties of preganglionic vagal cardiomotor neurones in the rabbit. *Pflügers Arch.* **395**, 244–250 (1982).
10. E. W. Taylor, M. S. Al-Ghamdi, I. H. Ihmied, T. Wang, A. S. Abe, The neuroanatomical basis of central control of cardiorespiratory interactions in vertebrates. *Exp. Physiol.* **86**, 771–776 (2001).
11. E. W. Taylor, C. A. C. Leite, M. R. Sartori, T. Wang, A. S. Abe, D. A. Crossley II, The phylogeny and ontogeny of autonomic control of the heart and cardiorespiratory interactions in vertebrates. *J. Exp. Biol.* **217**, 690–703 (2014).
12. E. W. Taylor, C. A. C. Leite, J. J. Levings, Central control of cardiorespiratory interactions in fish. *Acta Histochem.* **111**, 257–267 (2009).
13. S. W. Porges, *The Polyvagal Theory* (W.W. Norton and Co., 2013).
14. K. Johansen, Comparative Physiology: Gas exchange and circulation in fishes. *Annu. Rev. Physiol.* **33**, 569–612 (1971).
15. M. A. Biscotti, M. Gerdol, A. Canapa, M. Forconi, E. Olmo, A. Pallavicini, M. Barucca, M. Scharl, The lungfish transcriptome: A glimpse into molecular evolution events at the transition from water to land. *Sci. Rep.* **6**, 21571 (2016).
16. J. B. Graham, *Air Breathing Fishes: Evolution, Diversity, and Adaptation* (Academic Press, 1997).
17. A. F. Nogueira, C. M. Costa, J. Lorena, R. N. Moreira, G. N. Frota-Lima, C. Furtado, M. Robinson, C. T. Amemiya, S. Darnet, I. Schneider, Tetrapod limb and sarcopterygian fin regeneration share a core genetic programme. *Nat. Commun.* **7**, 13364 (2016).
18. D. J. McKenzie, H. A. Campbell, E. W. Taylor, M. Micheli, F. T. Rantin, A. S. Abe, The autonomic control and functional significance of the changes in heart rate associated with air breathing in the jeju, *Hoplerthyrinus unitaeniatus*. *J. Exp. Biol.* **210**, 4224–4232 (2007).
19. E. W. Taylor, H. A. Campbell, J. J. Levings, M. J. Young, P. J. Butler, S. Egginton, Coupling of the respiratory rhythm in fish with activity in hypobranchial nerves and with heartbeat. *Physiol. Biochem. Zool.* **79**, 1000–1009 (2006).
20. E. W. Taylor, Generation of the respiratory rhythm in fish, in *Encyclopedia of Fish Physiology: From Genome to Environment*, E. D. Farrell, Ed. (Elsevier, 2011), pp. 854–864.

21. E. Sandblom, A. Gräns, H. Seth, M. Axelsson, Cholinergic and adrenergic influences on the heart of the African lungfish *Protopterus annectens*. *J. Fish Biol.* **76**, 1046–1054 (2010).
22. S. Nilsson, On the autonomic nervous and chromaffin control systems of lungfish. *Aust. Zool.* **35**, 363–368 (2010).
23. M. Axelsson, A. S. Abe, J. Eduardo, P. W. Bicudo, S. Nilsson, On the cardiac control in the South American lungfish, *Lepidosiren paradoxa*. *Comp. Biochem. Physiol. A Physiol.* **93**, 561–565 (1989).
24. H. A. Campbell, E. W. Taylor, S. Egginton, The use of power spectral analysis to determine cardiorespiratory control in the short-horned sculpin *Myoxocephalus scorpius*. *J. Exp. Biol.* **207**, 1969–1976 (2004).
25. E. W. Taylor, T. Wang, Control of the heart and of cardiorespiratory interactions in ectothermic vertebrates, in *Cardio-Respiratory Control in Vertebrates*, M. L. Glass, S. C. Wood, Eds. (Springer, 2009), pp. 285–315.
26. A. P. Fishman, R. G. Delaney, P. Laurent, Circulatory adaptation to bimodal respiration in the dipnoan lungfish. *J. Appl. Physiol.* **59**, 285–294 (1985).
27. M. Bassi, H. Giusti, G. S. da Silva, J. Amin-Naves, M. L. Glass, Blood gases and cardiovascular shunt in the South American lungfish (*Lepidosiren paradoxa*) during normoxia and hyperoxia. *Respir. Physiol. Neurobiol.* **173**, 47–50 (2010).
28. M. Axelsson, in *Physiology and Biochemistry of the Fishes of the Amazon*, A. L. Val, V. M. F. de Almeida-Val, D. J. Randall, Eds. (Instituto Nacional de Pesquisas da Amazônia, 1996), pp. 213–229.
29. R. Fritsche, M. Axelsson, C. E. Franklin, G. G. Grigg, S. Holmgren, S. Nilsson, Respiratory and cardiovascular responses to hypoxia in the Australian lungfish. *Respir. Physiol.* **94**, 173–187 (1993).
30. K. Johansen, C. Lenfant, D. Hanson, Cardiovascular dynamics in the lungfishes. *Z. Vgl. Physiol.* **59**, 157–186 (1968).
31. K. Johansen, C. Lenfant, Respiration in the African lungfish *Protopterus aethiopicus*. *J. Exp. Biol.* **49**, 453–468 (1968).
32. E. W. Taylor, in *Fish Physiology* (Elsevier, 1992), vol. 12, pp. 343–387.
33. T. Wang, J. W. Hicks, W. K. Milsom, Changes in arterial O₂ content affect cardiac shunt but not ventilation in turtles. *Physiologist* **39**, A7 (1996).
34. T. Wang, E. W. Taylor, S. G. Reid, W. K. Milsom, Interactive effects of mechano- and chemo-receptor inputs on cardiorespiratory outputs in the toad. *Respir. Physiol. Neurobiol.* **140**, 63–76 (2004).
35. T. Wang, E. H. Krosnianas, J. W. Hicks, The role of cardiac shunts in the regulation of arterial blood gases. *Am. Zool.* **37**, 12–22 (1997).
36. G. V. Anrep, W. Pascual, R. Rössler, Respiratory variations of the heart rate. I—The reflex mechanism of the respiratory arrhythmia. *Proc. R. Soc. B. Biol. Sci.* **119**, 191–217 (1936).
37. Task Force, Heart rate variability: Standards of measurement, physiological interpretation, and clinical use. Task Force of the European Society of Cardiology and the North American Society of Pacing and Electrophysiology. *Eur. Heart J.* **17**, 354–381 (1996).
38. R. A. Neff, J. Wang, S. Baxi, C. Evans, D. Mendelowitz, Respiratory sinus arrhythmia: Endogenous activation of nicotinic receptors mediates respiratory modulation of brainstem cardioinhibitory parasympathetic neurons. *Circ. Res.* **93**, 565–572 (2003).
39. E. Agostoni, J. E. Chinnock, M. De Burgh Daly, J. G. Murray, Functional and histological studies of the vagus nerve and its branches to the heart, lungs and abdominal viscera in the cat. *J. Physiol.* **135**, 182–205 (1957).
40. J. S. Schwaber, D. H. Cohen, Electrophysiological and electron microscopic analysis of the vagus nerve of the pigeon, with particular reference to the cardiac innervation. *Brain Res.* **147**, 65–78 (1978).
41. S. Short, P. J. Butler, E. W. Taylor, The relative importance of nervous, humoral and intrinsic mechanisms in the regulation of heart rate and stroke volume in the dogfish *Scyliorhinus canicula*. *J. Exp. Biol.* **70**, 77–92 (1977).
42. D. J. Barrett, E. W. Taylor, The characteristics of cardiac vagal preganglionic motoneurons in the dogfish. *J. Exp. Biol.* **117**, 459–470 (1985).
43. A. Carravieiri, M. S. Müller, K. Yoda, S.-i. Hayama, M. Yamamoto, Dominant parasympathetic modulation of heart rate and heart rate variability in a wild-caught seabird. *Physiol. Biochem. Zool.* **89**, 263–276 (2016).
44. S. W. Porges, Love: An emergent property of the mammalian autonomic nervous system. *Psychoneuroendocrinology* **23**, 837–861 (1998).
45. H. A. Campbell, C. A. C. Leite, T. Wang, M. Skals, A. S. Abe, S. Egginton, F. T. Rantin, C. M. Bishop, E. W. Taylor, Evidence for a respiratory component, similar to mammalian respiratory sinus arrhythmia, in the heart rate variability signal from the rattlesnake, *Crotalus durissus terrificus*. *J. Exp. Biol.* **209**, 2628–2636 (2006).
46. J. Hayano, F. Yasuma, Hypothesis: Respiratory sinus arrhythmia is an intrinsic resting function of cardiopulmonary system. *Cardiovasc. Res.* **58**, 1–9 (2003).
47. L. A. Lipsitz, J. Mietus, G. B. Moody, A. L. Goldberger, Spectral characteristics of heart rate variability before and during postural tilt. Relations to aging and risk of syncope. *Circulation* **81**, 1803–1810 (1990).
48. N. D. Giardino, R. W. Glenny, S. Borson, L. Chan, Respiratory sinus arrhythmia is associated with efficiency of pulmonary gas exchange in healthy humans. *Am. J. Physiol. Heart Circ. Physiol.* **284**, H1585–H1591 (2003).
49. C. M. Masi, L. C. Hawkey, E. M. Rickett, J. T. Cacioppo, Respiratory sinus arrhythmia and diseases of aging: Obesity, diabetes mellitus, and hypertension. *Biol. Psychol.* **74**, 212–223 (2007).
50. J. Hayano, F. Yasuma, A. Okada, S. Mukai, T. Fujinami, Respiratory sinus arrhythmia: A phenomenon improving pulmonary gas exchange and circulatory efficiency. *Circulation* **94**, 842–847 (1996).
51. A. Ben-Tal, S. S. Shamailov, J. F. R. Paton, Evaluating the physiological significance of respiratory sinus arrhythmia: Looking beyond ventilation-perfusion efficiency. *J. Physiol.* **590**, 1989–2008 (2012).
52. M. L. Glass, S. C. Wood, K. Johansen, The application of pneumotachography on small unrestrained animals. *Comp. Biochem. Physiol. A Physiol.* **59**, 425–427 (1978).
53. S. Y. Lee, W. K. Milsom, The metabolic cost of breathing in red-eared sliders: An attempt to resolve an old controversy. *Respir. Physiol. Neurobiol.* **224**, 114–124 (2016).
54. T. Wang, S. J. Warburton, Breathing pattern and cost of ventilation in the American alligator. *Respir. Physiol.* **102**, 29–37 (1995).
55. S. G. Waxman, M. V. L. Bennett, Relative conduction velocities of small myelinated and non-myelinated fibres in the central nervous system. *Nat. New Biol.* **238**, 217–219 (1972).
56. B. L. Soloff, Buffered potassium permanganate-uranyl acetate-lead citrate staining sequence for ultrathin sections. *Stain Technol.* **48**, 159–165 (1973).
57. Z. Cheng, T. L. Powley, Nucleus ambiguus projections to cardiac ganglia of rat atria: An anterograde tracing study. *J. Comp. Neurol.* **424**, 588–606 (2000).
58. E. K. Corbett, T. F. Batten, J. C. Kaye, J. Deuchars, P. N. McWilliam, Labelling of rat vagal preganglionic neurones by carbocyanine dye DiI applied to the heart. *Neuroreport* **10**, 1177–1181 (1999).

Acknowledgments: This project benefited from a valuable collaboration with G. S. F. Silva [Universidade Estadual Paulista (UNESP)]. The authors are grateful to the Gonçalo Moniz Research Center, Oswaldo Cruz Foundation (CPQGM/FIOCRUZ, Salvador, Bahia, Brazil) for the use of its transmission electron microscope. We are also grateful to the Department of Genetics and Evolution of UFSCar (São Carlos, São Paulo, Brazil) and the Department of Biology of Biosciences Institute (UNESP, Rio Claro, São Paulo, Brazil) for the use of its fluorescence microscopes. Manipulators used to record from cardiac nerves were borrowed from S. Publicover, School of Biosciences, University of Birmingham, UK. **Funding:** This research was supported by Coordenação de Aperfeiçoamento de Pessoal de Nível Superior (postdoctoral fellowship to D.A.M.) and the National Institute of Science and Technology in Comparative Physiology (INCT-FisComp). E.W.T. was a senior visiting researcher under the Science Without Borders Program (CNPq 401061/2014-0). **Author contributions:** C.A.C.L. and E.W.T. conceived the study and designed the experiments; D.A.M. performed the experiments; M.R.S. and E.W.T. performed the neuroanatomy study; A.L.C. provided the TEM; D.A.M. analyzed the data; C.A.C.L. and F.T.R. provided support and supervised the project; E.W.T., D.A.M., and C.A.C.L. wrote the manuscript; all authors edited and commented on the manuscript. **Competing interests:** The authors declare that they have no competing interests. **Data and materials availability:** All data needed to evaluate the conclusions in the paper are present in the paper and/or the Supplementary Materials. Additional data related to this paper may be requested from the authors.

Submitted 29 September 2017

Accepted 19 January 2018

Published 21 February 2018

10.1126/sciadv.aqa0800

Citation: D. A. Monteiro, E. W. Taylor, M. R. Sartori, A. L. Cruz, F. T. Rantin, C. A. C. Leite, Cardiorespiratory interactions previously identified as mammalian are present in the primitive lungfish. *Sci. Adv.* **4**, eaaq0800 (2018).

Cardiorespiratory interactions previously identified as mammalian are present in the primitive lungfish

Diana A. Monteiro, Edwin W. Taylor, Marina R. Sartori, André L. Cruz, Francisco T. Rantin and Cleo A. C. Leite

Sci Adv 4 (2), eaaq0800.
DOI: 10.1126/sciadv.aaq0800

ARTICLE TOOLS	http://advances.sciencemag.org/content/4/2/eaaq0800
SUPPLEMENTARY MATERIALS	http://advances.sciencemag.org/content/suppl/2018/02/16/4.2.eaaq0800.DC1
REFERENCES	This article cites 51 articles, 10 of which you can access for free http://advances.sciencemag.org/content/4/2/eaaq0800#BIBL
PERMISSIONS	http://www.sciencemag.org/help/reprints-and-permissions

Use of this article is subject to the [Terms of Service](#)

Science Advances (ISSN 2375-2548) is published by the American Association for the Advancement of Science, 1200 New York Avenue NW, Washington, DC 20005. 2017 © The Authors, some rights reserved; exclusive licensee American Association for the Advancement of Science. No claim to original U.S. Government Works. The title *Science Advances* is a registered trademark of AAAS.